Autism-linked CHD gene expression patterns during development predict multi-organ disease phenotypes

Sahrunizam Kasah*, Christopher Oddy* & M. Albert Basson^

Centre for Craniofacial and Regenerative Biology, King's College London, Floor 27, Guy's Hospital Tower Wing, London SE1 9RT, UK and MRC Centre for Neurodevelopmental Disorders, King's College London, London SE1 1UL, UK.

*Joint first authors

^Correspondence:

Dr. M.A. Basson

Centre for Craniofacial and Regenerative Biology King's College London

Floor 27, Guy's Hospital Tower Wing

London SE1 9RT

UK

Tel: +44-207 188 1804

email: albert.basson@kcl.ac.uk

Keywords: CHD2, CHD7, CHD8, expression, mouse, autism, embryo, development, organogenesis

Short title: CHD gene expression during mouse development

Abstract

Recent large-scale exome sequencing studies have identified mutations in several members of the CHD (Chromodomain Helicase DNA-binding protein) gene family in neurodevelopmental disorders. Mutations in the *CHD2* gene have been linked to developmental delay, intellectual disability, autism and seizures, *CHD8* mutations to autism and intellectual disability, whereas haploinsufficiency of *CHD7* is associated with executive dysfunction and intellectual disability. In addition to these neurodevelopmental features, a wide range of other developmental defects are associated with mutants of these genes, especially with regards to *CHD7* haploinsufficiency, which is the primary cause of CHARGE syndrome. Whilst the developmental expression of *CHD7* has been reported previously, limited information on the expression of *CHD2* and *CHD8* during development is available. Here we compare the expression patterns of all three genes during mouse development directly. We find high, widespread expression of these genes at early stages of development that gradually becomes restricted during later developmental stages. *Chd2* and *Chd8* are widely expressed in the developing central nervous system (CNS) at all stages of development, with moderate expression remaining in the neocortex, hippocampus, olfactory bulb and cerebellum of the postnatal brain. Similarly, *Chd7* expression is seen throughout the CNS during late embryogenesis and early postnatal development, with strong enrichment in the cerebellum, but displays low expression in the cortex and neurogenic niches in early life. In addition to expression in the brain, novel sites of *Chd2* and *Chd8* expression are reported throughout the developing mouse. These findings suggest additional roles for these genes in organogenesis and predict that mutation of these genes may predispose individuals to a range of other, non-neurological developmental defects.

Introduction

Chromatin remodelling factors have emerged as key regulators of gene expression and are often mutated in human disease (Iwase et al, 2018; Hendrich and Bickmore, 2001; Ronan, Wu & Crabtree et al, 2013). Mammalian chromatin remodelling factors can be subdivided into four families: SWI/SNF (mating type Switching/Sucrose Non-Fermenting), ISWI (Imitation Switch), INO80 (Inositol requiring 80) and CHD (Chromodomain Helicase DNA-binding protein) (Ho and Crabtree, 2010).

The CHD gene family consists of nine genes (*CHD1-CHD9*). The encoded proteins utilise the energy from ATP hydrolysis to alter nucleosome positioning, thereby causing local changes in the structure of the chromatin (Marfella & Imbalzano, 2007). CHD1 and CHD2, which belong to CHD1-2 subfamily, are characterised by the presence of tandem chromodomains and a Snf2 helicase domain – both motifs common to all CHD proteins – in addition to DNA-binding domains at the C-terminus (Marfella & Imbalzano, 2007; Liu, Ferreria & Yusufzai, 2015). CHD3 and CHD4 are structurally similar but each contain a PHD (Plant Homeo Domain) Zn-finger-like domain rather than a DNA binding region, forming the second subfamily (Marfella & Imbalzano, 2007). Alongside signature sequence motifs of the CHD family, members of the CHD5-9 subfamily contain a DNA binding region alongside various other C-terminal sequences that alter their function (Marfella & Imbalzano, 2007). The present study focuses on the spatiotemporal pattern of expression of CHD2, CHD7 and CHD8.

The ATP-dependent activity of CHD2 leads to assembly of chromatin into periodic nucleosome arrays by deposition of various histone proteins, thereby modifying the expression and structure of target sites (Liu, Ferreria & Yusufzai, 2015; Luijsterburg et al., 2016). Functionally, CHD2 has been reported to maintain pluripotency of stem cells, influence cell fate during myogenesis and interneuron development and facilitate DNA repair through interaction with histone variant H3.3 (Harada et al, 2012; Luijsterburg et al., 2016; Meganathan et al, 2017; Rajagopalan, Nepa & Venkatachalam et al., 2012; Semba et al, 2017).

De novo loss-of-function mutations in *CHD2* have been reported in Autism Spectrum Disorder (ASD) patients alongside developmental delay, intellectual disability, increased risk of epileptic seizures and additional behavioural problems (Allen et al, 2013; Chérnier et al, 2014; Lebrun et al, 2017; O'Roak et al, 2014; Pinto et al, 2016). The association between *CHD2* haploinsufficiency and epileptic encephalopathy, or Lennox-Gastaut or Dravet syndrome, is also well-established and variants of *CHD2* are recognised risk factors for photosensitivity in epilepsy (Carvill et al, 2013; Galizia et al, 2015; Lund et al, 2014; Suls et al, 2013). *CHD2* mutations are commonly identified in patients with chronic lymphocytic leukaemia, frequently in conjuncture with alterations in functional pathways associated with brain development (Rodríguez et al, 2015).

Homozygous *Chd2* mutant mice die around birth due to unknown causes (Marfella et al, 2006). Heterozygous mice exhibited reduced growth and viability and range of phenotypic abnormalities which include extramedullary haematopoiesis, susceptibility to lymphomas, cardiomyopathy, liver inflammation, glomerulopathy and various other renal defects (Marfella et al, 2006; Marfella et al, 2008; Nagarajan et al, 2009; Rajagopalan, Nepa & Venkatachalam et al., 2012). More recently *Chd2* knockdown has been demonstrated to decrease $Pax6^{+}$ radial glial cell numbers, a cell type in which it is highly expressed, and to promote neuronal and intermediate progenitor production, implying an important balancing role for CHD2 in progenitor renewal and cortical development (Shen et al, 2015). At present limited expression data for *Chd2* is available. Quantitative analyses of *Chd2* in the adult mouse demonstrate that *Chd2* is widely expressed by a multitude of functional tissue groups including the heart, brain, lungs, thymus, lymphoid tissue and skeletal muscle (Marfella et al, 2006; Nagarajan et al, 2009). Macroscopic analysis of whole embryos stained for *Chd2* showed expression in the developing heart, forebrain, eye, dorsal facial region and limbs between E10.5 and E15.5 (Kulkarni et al, 2008). These data show that *Chd2* expression is apparent in many tissues during development and in the adult mouse although a true spatiotemporal pattern of expression is yet to be defined.

CHD7 is thought to maintain an open chromatin conformation at putative regulatory elements (Feng et al, 2017; Whittaker et al, 2017b). CHD7 facilitates neural stem cell (NSC) multipotency in the developing brain and quiescence in the adult as both differentiation potential and stem cell depletion rates are correlated with the levels of CHD7 (Feng et al, 2015; Fujita, Ogawa & Ito, 2016; Jones et al, 2015; Yamamoto et al, 2018). As well as maintaining multipotency, CHD7 has also been shown to directly control lineage identity in NSCs through coordination of transcription factors in the neural crest (Chai et al, 2018). In a similar vein, CHD7 is required for the formation of migratory neural crest cells and, accordingly, induced pluripotent stem cells (iPSCs) derived from patients with CHD7 mutations exhibit defective delamination, migration and motility (Bajpai et al, 2010; Prasad et al, 2012; Okuno et al, 2017). Finally, CHD7 has been shown to have multiple roles in cerebellar development; consistent with the observation that individuals harbouring CHD7 mutations may exhibit vermis hypoplasia (Yu et al, 2013; Whittaker et al, 2017a; Whittaker et al, 2017b; Donovan et al, 2017).

Haploinsufficiency of the *CHD7* gene is the major cause of CHARGE syndrome (Coloboma of the eye, Heart defects, Atresia of the choanae, Retardation of growth and/or development, Genitalia and/or urinary abnormalities and Ear abnormalities and deafness) and mutations have also been reported in patients with Kallmann syndrome (Jongmans et al, 2009; Kim et al, 2008). Some of the *CHD7* mutations in patients with CHARGE syndrome have been shown to result in defective nucleosome remodelling activity in-vitro, directly linking chromatin remodelling defects with disease (Bouazoune and Kingston, 2012). *Chd7*$^{-/-}$ embryos do not survive beyond E11, indicating early requirements for this gene during embryonic development, whereas heterozygotes exhibit features similar to those associated with CHARGE syndrome (Bosman et al, 2005; Hurd et al, 2007). Akin to *Chd2*, *Chd7* expression during development is not limited to one tissue type. *Chd7* has been shown to be expressed in the developing eye, inner ear, olfactory epithelium, dorsal root ganglia, lung, kidneys, gut and throughout the neural ectoderm, including the neural crest (Aramaki et al, 2007; Bosman et al, 2005; Engelen et al, 2011; Fujita et al, 2014; Fujita Ogawa & Ito, 2016; Gage, Hurd & Martin, 2015; Hurd et al, 2007). More recently, preserved expression of *Chd7* has been seen in the adult cerebellum (Whittaker et al, 2017a).

In vitro evidence has suggested a central role of CHD8 in transcription and transcriptional elongation (Nishiyama et al, 2009; Rodriguez-Paredes et al, 2009; Yates et al, 2010; Yuan et al, 2007). CHD8S, a partial N-terminal fragment of CHD8, also referred to as Duplin, acts as a regulator of β-catenin mediated transcription – largely causing transcriptional repression (Durak et al, 2016; Kobayashi et al, 2002; Nishiyama, 2004; Nishiyama et al, 2012; Platt et al, 2017; Sakamoto et al, 2000; Thompson et al, 2008).

Recurrent de novo mutations in *CHD8* have been linked to ASD. A significant body of literature, including case reports and large exome sequencing studies, have identified *CHD8* mutations in individuals with ASD (Bernier et al, 2014; Neale et al, 2012; Merner et al, 2016; O' Roak et al, 2012; Sanders et al, 2012; Stolerman et al, 2016; Talkowski et al, 2012; Wang et al, 2016; Wilkinson et al, 2015; Zahir et al, 2007). It is one of the highest confidence risk genes for autism identified to date. ASD is highly heterogeneous but can be identified by a repertoire of behavioural features in patients: social impairment, communication impairment, repetitive behaviours and sometimes accompanied by an array of other conditions such as epilepsy, dyslexia, dyspraxia and attention deficit hyperactivity disorder (ADHD) (Brieber et al, 2007; Canitano, 2007; Dziuk et al, 2007; Helbig et al, 2009; Leyfer et al, 2006; Taurines et al, 2012). The effects of *CHD8* mutation may also manifest as characteristic physical features including macrocephaly, facial dysmorphia and gastrointestinal disturbance, perhaps defining *CHD8*-related ASD as a distinct subtype (Bernier et al, 2014).

CHD8 is recruited to promoters of highly expressed genes in NSCs and reduced expression of CHD8 in mouse and human cells has been shown to precipitate dysregulation of ASD related genes and alter cortical neurogenesis (Cotney et al, 2015; Durak et al, 2016; Sugathan et al, 2014; Wang et al, 2015; Wilkinsion et al, 2015). In *Chd8*$^{+/-}$ mice behavioural changes have been documented alongside characteristic neurodevelopmental changes pertaining to altered neurogenesis and long-range connectivity, brain overgrowth and craniofacial anomalies (Gompers et al, 2017;

Katayama et al, 2016; Platt et al, 2017; Suetterlin et al, 2018). *Chd8*$^{-/-}$ embryos die by E7.5 of development. The early embryonic lethality associated with CHD8 loss has been proposed to be caused by aberrant p53-mediated apoptosis as a consequence of loss of CHD8-mediated repression of p53 target genes (Nishiyama et al, 2004). As the mutants do not survive, the developmental roles after E7.5 are not known. The expression pattern of *Chd8* has been described between E7.5 and E10.5 in the mouse using a CHD8s/Duplin antisense riboprobe (Nishiyama et al, 2004). Whole embryo analysis showed expression predominantly in the brain, face and limb buds. Since, microarray data has been used to quantify the level of *Chd8* expression in developing mouse, macaque and human brains. A regional expression heatmap showed widespread expression, highest in the early pre-natal period (Bernier et al, 2014). Platt et al (2017) demonstrated a similar temporal pattern of quantitative expression in the mouse brain and further showed that *Chd8* is expressed in almost all neuronal populations. Despite these insights, no study to date has characterised the macroscopic expression pattern of *Chd8* in all tissues of the developing mouse from mid-gestation and through early life. Given the strong association of CHD8 mutations with ASD and other physical abnormalities, determining a comprehensive spatiotemporal expression pattern of CHD8 during development is of great interest.

In the present study, we investigated the spatiotemporal patterns of three CHD genes with strong evidence for important functions in brain development and neurodevelopmental disorders. The expression pattern of *Chd8* was compared with *Chd7* and *Chd2*. As these genes tend to be widely expressed during early development, we focused on later embryonic stages to identify novel expression sites during organogenesis. We report novel expression sites for all three genes during development, with examples of overlapping, complementary and distinct expression patterns.

Material and Methods

Animals

Timed-mated CD1 embryos and pups were produced in our in-house facility. Noon on the day a vaginal plug was detected was designated as embryonic day 0.5 (E0.5). The day of birth was designated as postnatal day (P)0. All experimental procedures were approved by the institutional Local Ethical Review Panel and the UK Home Office.

Primer design and probe synthesis

Primers were designed to amplify a 455 bp fragment of exon 37 of *Chd8* from mouse genomic DNA: forward 5'-TCTCTGCCTTTTATGCCGTTTG-3'; reverse 5'-CACCTCCTGAAGTCTTGGGTTTC-3' with T7 recognition sequence added to the reverse primers in a PCR reaction. The resulting DNA template was used for the synthesis of digoxigenin (DIG)-labelled antisense or sense mRNA probes. A *Chd7* probe template was made with primer pairs that amplify a 222 bp fragment of *Chd7* exon 3 from mouse genomic DNA: forward 5'-TTGGTAAAGATGACTTCCCTGGTG-3'; reverse 5'-GTTTTGGCGTGACAGTTTTTGC-3'. A *Chd2* 625bp probe template was amplified from mouse brain cDNA using primer pairs: forward 5'-AGAAGAGCGTCCTCACAAAGACTG-3'; reverse 5'-TTTTTCCTCAGGGTCCACAGG-3'.

Sample preparation

Embryos and brains were dissected in ice-cold diethylpyrocarbonate-treated phosphate buffered saline (DEPC PBS) and fixed in 4% paraformaldehyde (PFA) overnight. After several washes in DEPC PBS, embryos or brains were placed in cassettes immersed in 70% ethanol. The samples were processed in a Leica ASP300 tissue processor following a standard protocol. The processed samples were embedded in wax, sectioned sagittally at 10 µm using a Leica RM2145 microtome, placed on Superfrost Plus slides and left to dry at 42°C for 48 hours.

In situ hybridisation

E12.5, E14.5, P0, P7 and P20 sagittal sections on slides were deparaffinised in Xylene and rehydrated in decreasing series of ethanol concentrations. This was followed by DEPC PBS washes. Proteinase K (50 µg/ml in DEPC PBS) was added and sections were incubated for 10 minutes at 37 °C.

The slides were then washed in DEPC PBS, refixed in 4% PFA for 10 minutes and washed again in DEPC PBS. Sections were acetylated (acetic anhydride, 0.1M Triethanolamine, DEPC water at pH 7.5) for 10 minutes after which they were again washed in DEPC PBS thrice. Sections were dehydrated in 70% ethanol (5 minutes) and 95% ethanol (a few seconds) and left to air dry for a few minutes. 300 µl probe-hybridisation mix (2 µl of probe per ml hybridisation solution) (50% Dextran Sulfate, 50% Formamide, 1% Denhardts solution, 0.3M NaCl (sodium chloride), 20mM Tris-HCl (pH8), 10mM $NaPO_4$ (sodium phosphate), 5mM EDTA (Ethylenediaminetetraacetic acid), 250µg/ml Yeast tRNA, 1% sarcosyl, sterile water) pre-heated to 80°C were added to each slide and covered with parafilm. The slides were then arranged in a humid chamber (50% formamide/water) and incubated overnight at 65°C.

The following day the slides were washed in high stringency (HIS) (formamide, 0.1% SSC (saline-sodium citrate), sterile distilled water) wash for 30 minutes at 65°C followed by RNase buffer (0.5M NaCl, 10mM Tris-HCl pH 7.5, 5mM EDTA, distilled water) at 37 °C for 10 minutes (3x). Slides were treated with RNase buffer with 20 µg/ml RNase A at 37°C for 30 minutes followed by a single wash in RNase buffer at 37°C for 15 minutes. The slides were again washed twice in HIS at 65°C for 20 minutes each. 2x SSC and 0.1x SSC washes for 15 minutes were performed twice followed by PBT (PBS, 0.1% Tween 20) washes at room temperature. Sections were blocked with 10% heat inactivated goat serum in PBT for one hour at room temperature before a 3-hour incubation in alkaline phosphatase coupled with anti-dioxygenin antibody (1:500 dilution, Roche) and 1% heat-inactivated goat serum in PBT. At the end of incubation, slides were washed four times with PBT for 15 minutes each at room temperature followed by freshly prepared NTMT buffer (5M NaCl, 1M Tris-HCl at pH 9.5, 1M

MgCl$_2$, 0.1% Tween-20, sterile distilled water and 0.5 mg/ml levamisole) twice at room temperature. Finally, the slides were incubated in darkness in BM purple (Roche) and 0.5 mg/ml levamisole at room temperature overnight.

When signal appeared on sections, the reaction was stopped by washing in PBS at room temperature for 5 minutes. Slides were dehydrated with an increasing series of ethanol washes followed by Xylene before being mounted with Di-N-Butyle Phthalate in Xylene (DPX) and left to air dry.

Results

Chd2, *Chd7* and *Chd8* gene expression in mouse embryos at E12.5 and E14.5.

At E12.5 *Chd7* and *Chd8* expression was apparent throughout the neuroepithelium of the developing central nervous system (CNS) (Figure 1A, B). *Chd8* transcript signals were observed throughout the ventricular and subventricular regions of the neocortex and in the hindbrain (Figure 1Aa, Ab), including the cerebellum where expression was evident in the ventricular zone (VZ), rhombic lip (RL) and the isthmus (Figure 1Aa). Both VZ and RL are germinal centres where progenitor cells are born that later migrate and populate the cerebellum (White and Sillitoe, 2012). Notably, *Chd8* expression could also be observed at the lower rhombic lip and floor plate region of the hindbrain, extending to the spinal cord and dorsal root ganglia (Figure 1A, Supplementary Figure 1A). *Chd8* expression can be observed throughout the neural tube with no evident mediolateral nor dorsoventral gradient (Supplementary Figure 1A-D). Other regions of interest showing high *Chd8* expression included the diencephalon and areas adjacent to the hypothalamus and pituitary gland (Figure 1A). *Chd8* expression was observed throughout the craniofacial region including the tongue and olfactory epithelium (Figure 1A). Elsewhere, other organs of the embryo also showed substantial *Chd8* expression with signals present in the intersomitic regions, lungs, gut, genital tubercle and tail (Figure 1A).

As with *Chd8*, *Chd7* mRNA transcripts were observed throughout the embryo (Figure 1B). Expression was found in the ventricular region of the developing brain and spinal cord. *Chd7* mRNA transcripts were present in both the ventricular and subventricular zones of the neocortex (Figure 1Bb). In the hindbrain, *Chd7* was expressed in all regions including the upper rhombic lip of the cerebellum, the lower rhombic lip and floor plate (Figure 1Ba). *Chd7* expression was also observed in the diencephalon and the pituitary (Figure 1B). Within the neural tube expression was present in both cranial and caudal poles (Supplementary Figure 1E, F). Additionally, in transverse sections *Chd7* at this stage was noted to be enriched in the ventricular zone and displayed a

ventral to dorsal gradient within the developing spinal cord (Supplementary Figure 1G, H). Extensive expression was also observed outside the CNS. In the head region, diffuse *Chd7* expression was present in the tongue. Other organs with expression included the dorsal root ganglia, intersomitic regions, gut, lungs, and the tail (Figure 1B).

At E12.5, *Chd2* mRNA transcript signals could be found in many tissues in the developing mouse (Figure 1C), differentiated from background by use of a sense control (Supplementary Figure 2). Diffuse *Chd2* expression was observed within the brain (Figure 1Ca, Cb), intersomitic regions and the spinal cord. Despite this increased signal density in brain tissue, the level of expression compared to other regions was low, suggesting that, at this stage, *Chd2* is expressed ubiquitously at low levels throughout the embryo.

As several tissues outside of the CNS expressed both *Chd7* and *Chd8* strongly, these were compared directly at higher power. Sites of expression included the cochlea, lungs, eyes and kidneys (Figure 2A-D, F-I). For both, distinct expression levels were observed at the vestibulocochlear ganglion and cochlear epithelium in the ear (Figure 2A, F). In the kidney, expression levels were high in the mesenchyme and metanephric tubule epithelium (Figure 2B, G) whereas in the lung, expression was observed in the pulmonary epithelium (Figure 2C, H). Both transcripts were also observed in the neural retina/optic cup and retinal pigmented epithelium of the eyes, with *Chd8* transcripts present widely throughout the surrounding mesenchyme and craniofacial tissues (Figure 2D, I). Interestingly, *Chd8* also showed high expression in the incisor primordium, where no *Chd7* expression was seen (Figure 2E).

In E14.5 embryos, several sites of prominent *Chd8* expression could be seen (Figure 3A). In the head, abundant *Chd8* transcripts were observed in the forebrain, midbrain, rhombic lip and ventricular zone of the cerebellum (Figure 3Aa). In the neocortex, significant expression was revealed in the ventricular, subventricular and mantle zones (Figure 3Ab). Prominent expression was also seen in the basal forebrain, including the ganglionic eminences, suggesting a role for *Chd8* in the generation of GABA-ergic

interneurons (Figure 3A). Diffuse or low *Chd8* expression was observed in the diencephalon and midbrain region. Extending from the hindbrain region, the spinal cord also showed low expression. Elsewhere in the head, expression was seen in the olfactory epithelium, the tongue and the ventral incisor. Other organs continued to show *Chd8* expression as at E12.5, including the lungs, gut and kidneys. In addition, at E14.5, *Chd8* transcripts were detected within the heart, thyroid, thymus, liver, gastric epithelium, trigeminal ganglion and digits of the hind limb (Figure 3A).

Comparable to its expression at E12.5, high levels of *Chd7* mRNA transcripts were present most prominently in the ventricular region of the neocortex (Figure 3Bb) in accordance with previous expression analyses (Engelen et al, 2011). Signals were also observed in the midbrain region extending to the hindbrain (Figure 3B). Within the cerebellum, significant *Chd7* signals were observed at the rhombic lip and ventricular zone of the fourth ventricle (Figure 3Ba). Widespread *Chd7* expression was also present in the diencephalon (Figure 3B). Extending from the hindbrain, the spinal cord showed widespread *Chd7* signal. In the oral region, the tongue and incisor primordium showed *Chd7* expression. Note that its expression in the tooth appears to occur later in development, at E14.5, than its family member *Chd8* (Figure 2J). Other organs such as the lungs, thymus, heart, kidneys and liver, which showed significant *Chd8* expression, also displayed *Chd7* expression (Figure 3B).

Chd2 expression at E14.5 was still low and widespread but was markedly elevated in certain regions compared to E12.5 (Figure 3C). Strong signals were detected in the neocortex (Figure 3Cb) and rhombic lip of the cerebellum (Figure 3Ca), enriched in the ventricular zone of the cerebellum. In the craniofacial region the tongue, incisor primordium and olfactory epithelium all stained for *Chd2*. Specific expression signals outside of the head were noted in the kidney, liver, thymus, lung, thyroid, gut, digits of the hindlimb and myogenic tissue (Figure 3C).

Much like at E12.5, both *Chd8* and *Chd7* transcripts could be detected in the kidneys, lungs and eyes (Figure 3Ac-Ae, Bc-Be). Additionally, however a strong *Chd2* signal

could also be detected in these tissues at this stage (Figure 3Cc-Ce). mRNA transcripts of all three genes were detected at the condensing mesenchyme of the kidney (Figure 3Ae, Be, Ce), epithelium of the lung (Figure, 3Ad, Bd, Cd) and neural retina, optic cup and lens of the eyes, with particularly strong expression of *Chd7* seen in the retina (Figure, 3Ac, Bc, Cc). Notably, a *Chd2* signal was also detected in the anatomical space containing the optic nerve and its surrounding structures at this stage (Figure 3Cc).

Distinct *Chd2*, *Chd7* and *Chd8* expression patterns in the postnatal mouse brain

In order to define the domains of *Chd8* expression in the postnatal brain, in situ hybridisation on brain sections at P0 were carried out. At this stage, widespread expression of *Chd8* was observed (Figure 4A, A'), in agreement with previous studies suggesting that *Chd8* expression peaks during mid-gestation in the embryo (Bernier et al, 2014; Platt et al, 2017). Closer examination revealed expression throughout the cerebellum (Figure 4Aa) and a slight enrichment of *Chd8* expression towards the outer neocortex (Figure 4Ab). Other *Chd8*-expressing regions of interest include the hippocampus, hypothalamus and olfactory bulb (Figure 4A, A').

At this stage, a comparable widespread pattern of expression was seen for *Chd7* (Figure 4B, B', C, C') with *Chd7* exhibiting particularly strong expression in the cerebellum and pons (Figure 4Ba, Ca). *Chd7* was highly expressed within the cerebellum in contrast to *Chd2* and *Chd8* for which moderately strong and more diffuse expression was seen (Figure 4Aa-Ca). *Chd2* transcripts were enriched in the outer neocortex, hypothalamic area, superior olivary complex and basal pons (Figure 4C).

The expression patterns of these genes in the P7 brain were similarly widespread with continued expression in the cerebellum, neocortex and hippocampus (Figure 5A-C, A'-C'). Interestingly, all three genes appear to be expressed within the rostral migratory

stream (RMS) suggesting a role for the CHD family in coordinating the formation of the infant olfactory system. High power images demonstrated prominent expression of all three genes in the cerebellum (Figure 5Aa-Ca), the dentate gyrus (DG) and cornu ammonis 1-3 (CA1-3) of the hippocampus (Figure 5Ab- Cb) and neocortex, enriched in layers II-III of the neocortex (Figure 5Ac- Cc). This cortical distribution is particularly marked for both *Chd7* and *Chd8* where a distinct band of high signal density can be appreciated. Much like in the P0 brain, *Chd7* was most strongly expressed in the cerebellum.

At P20, *Chd8* and *Chd2* expression was prominent in the cerebellum, neocortex, hippocampus, RMS and olfactory bulb (Figure 6A, A', C, C'). *Chd7* was most prominent in the cerebellum, with low expression in the hippocampus, RMS and olfactory bulb (Figure 6B, B', Bc). All three genes were expressed in the maturing granule cell layer (GCL) of the cerebellum (Figure 6Aa-Ca) and the DG and CA1-3 of the hippocampus (Figure 6Ab-Cb). *Chd2* and *Chd7* expression in the hippocampus was much lower and more diffuse compared to the prominent expression of *Chd8* (Figure 6Ab-Cb). Clear expression of *Chd2* and *Chd8* was noted in the neocortex, whilst *Chd7* expression was very low in comparison (Figure 6Ac-Cc).

Discussion

The results of the current study demonstrate that all three genes are widely expressed and show little evidence of restricted temporal and spatial expression patterns during embryonic development. Although expression seemingly occurs in many different tissues in-utero it can be noted that neurological tissue in particular expresses these members of the CHD family at a high level; an observation that is not wholly unsurprising considering the phenotypic manifestations of mutations of these genes.

CHD gene expression in the embryo

Chd8 is widely expressed in embryonic stages E12.5 and E14.5, consistent with a continued role for CHD8 during early stages of development, after E7.5 when *Chd8*$^{-/-}$ mouse embryos were demonstrated to die due to apoptosis (Nishiyama et al, 2004). Recent work also implicated a role for CHD8 in suppressing p53 and the transactivation of genes under p53 control by preventing the process of apoptosis (Nishiyama et al, 2009). This could explain the early embryonic lethality observed. Moreover, the suggested role of CHD8 in transcription and elongation together with its role in controlling the expression of CCNE2 and TYMS which are involved in the G1/S phase of cell cycle reinforce its possible role in normal gene regulation and cell proliferation respectively (Rodriguez-Paredes et al, 2009), hence normal development.

Similar to *Chd8*, the widespread *Chd2* and *Chd7* expression suggests they also have important roles in early developmental processes and organogenesis. These data are consistent with the evidence that neither *Chd2* nor *Chd7* homozygotes thrive past early development (Bosman et al, 2005; Hurd et al, 2007; Marfella et al, 2006). The *CHD7* gene is the dominant cause of CHARGE syndrome which is characterised by defects in the eye, brain, ear, heart and genitalia; areas in which we observed high levels of *Chd7* expression (Janssen et al, 2012; Vissers et al, 2004). There are also reports of scoliosis caused by *CHD7* mutations (Gao et al, 2007) which might relate to the expression we observed in the inter-somitic mesoderm. FAM124B was reported to be a component of a CHD7 and CHD8-containing complex (Batsukh et al, 2012) suggesting that this multi-protein complex could be functional in cells where *Chd7* and *Chd8* are co-expressed. Whereas *CHD7* mutations are clearly linked to multi-organ defects in the context of CHARGE syndrome (Gao et al, 2007; Janssen et al, 2012; Patten et al, 2012; Van de Laar et al, 2007; Vissers et al, 2004), a clear role for CHD8 in organogenesis has not been reported. Here, however, we show that *Chd8* is expressed in many developing organs including the lumen of stomach and midgut; an observation which may explicate the gastrointestinal complications associated with *CHD8* mutations in ASD patients (Bernier et al, 2014).

In the case of *Chd2*, heterozygous mice most notably display an array of gross kidney abnormalities, which might pertain to the high levels of expression of this gene we

observed in the developing kidney (Marfella et al, 2008). Despite this association, the absence of reported renal dysgenesis in humans harbouring *CHD2* mutations might indicate divergent functions for this gene in the human kidney, or a degree of functional redundancy with other CHD genes. Notably, at E14.5 the *Chd2* expression pattern was markedly similar to *Chd8* and indeed, several regions of the embryo at this stage expressed these two genes in exclusion of *Chd7*, suggesting the possibility that they may serve similar functions. Some such regions include the dorsal hindlimb, thyroid, gut and olfactory epithelium.

CHD genes in brain development

CHD2 and *CHD8* mutations share a well-established link with ASD, a disorder that is widely regarded to be caused by aberrant neurodevelopment (Lebrun et al, 2017; O' Roak et al, 2012; Neale et al, 2012; Sanders et al, 2012). Our study demonstrates high levels of both *Chd2* and *Chd8* expression in the developing brain, especially during embryonic development. Additionally, preserved expression of both was revealed in key areas of the perinatal (P0) and postnatal brain (P7 and P20) including the cerebellum, hippocampus and neocortex – regions of the brain that are implicated in ASD (Allen, 2005; de Anda et al, 2012; Donovan & Basson, 2017; Riedel and Micheau, 2001). Within the neocortex expression of *Chd2* and *Chd8* appears to be particularly prominent within the outer layers, distinctly layers II-III of the postnatal brain, areas in which high numbers of other ASD risk genes are also enriched (Parikshak et al, 2013).

Taken together, and bolstered by evidence of aberrant neurodevelopmental phenotypes associated with mutants of these genes (Allen et al, 2013; Chérnier et al, 2014;Gompers et al, 2017; Katayama et al, 2016; Lebrun et al, 2017; O'Roak et al, 2014; Pinto et al, 2016; Platt et al, 2017; Suetterlin et al, 2018), our data suggest that *Chd2* and *Chd8* are expressed in a spatiotemporally appropriate way such that impairment in their expression might precipitate some of the neurological changes seen in patients with ASD. With both genes expressed in the SGZ of the hippocampus our data further support the notion that CHD2 and CHD8 might regulate neurogenesis (Shen et al, 2015; Durak

et al, 2016), akin to the reported role of their counterpart CHD7 (Feng et al, 2013; Jones et al, 2015).

In addition to its role in adult neurogenesis, the diverse, temporally distinct functions of CHD7 during cerebellar development (Yu et al, 2013; Whittaker et al, 2017a; Whittaker et al, 2017b; Donovan et al, 2017), are consistent with its pronounced expression in the postnatal cerebellum. In view of the role of CHD7 in neurodevelopment our study supports the notion that its mutation might account for the cerebellar hypoplasia associated with CHARGE syndrome. Furthermore, its expression in the olfactory bulb and RMS throughout postnatal development further bolsters the link between Kallmann syndrome, characterised by anosmia and hypogonadism, and CHD7 mutation (Jongmans et al, 2009).

Finally, the reported expression of *Chd2* in the postnatal hippocampus invites a potential link between the dysfunction and deficiency of hippocampal interneurons documented in epileptic encephalopathies, temporal lobe epilepsy and seizures associated with ASD and its proposed role in interneuron development (Fyre et al, 2016; Lado et al, 2013; Liu et al, 2014; Meganathan et al, 2017). Furthermore, *Chd2* expression in the eye and related structures during early development might also pertain to the association of *CHD2* mutation with photosensitivity in epilepsy (Carvill et al, 2013; Galizia et al, 2015; Lund et al, 2014; Suls et al, 2013).

In conclusion, in addition to their established roles in early brain development, our expression analyses also implicate *Chd2* and *Chd8*, alongside *Chd7*, in organogenesis. Our data also implicate all three genes in the process of postnatal neurogenesis due to their expression in the neurogenic niches of the adult brain. Additional studies will be necessary to further define the function of these genes in these developmental processes. The gene expression data reported here will provide invaluable information and reference points to guide these future studies.

Acknowledgements

This work was supported by an Anatomical Society Undergraduate Summer Vacation Scholarship to CO.

References

Allen G, McColl R, Barnard H, et al. (2005) Magnetic resonance imaging of cerebellar-prefrontal and cerebellar-parietal functional connectivity. Neuroimage, 28, 39-48.

Aramaki M, Kimura T, Udaka T, et al. (2007) Embryonic expression profile of chicken CHD7, the ortholog of the causative gene for CHARGE syndrome. Birth Defects Res A Clin Mol Teratol, 79, 50-57.

Bajpai R, Chen DA, Rada-Iglesias A, et al. (2010) CHD7 cooperates with PBAF to control multipotent neural crest formation. Nature, 463, 958-962.

Batsukh T, Pieper L, Koszucka AM, et al. (2010) CHD8 interacts with CHD7, a protein which is mutated in CHARGE syndrome. Hum Mol Genet, 19, 2858-2866.

Batsukh T, Schulz Y, Wolf S, et al. (2012) Identification and characterization of FAM124B as a novel component of a CHD7 and CHD8 containing complex. PLoS One, 7, e52640.

Bernier R, Golzio C, Xiong B, et al. (2014) Disruptive CHD8 mutations define a subtype of autism early in development. Cell, 158, 263-276.

Bosman EA, Penn AC, Ambrose JC, et al. (2005) Multiple mutations in mouse Chd7 provide models for CHARGE syndrome. Hum Mol Genet, 14, 3463-3476.

Bouazoune K, Kingston RE (2012) Chromatin remodeling by the CHD7 protein is impaired by mutations that cause human developmental disorders. Proc Natl Acad Sci U S A, 109, 19238-19243.

Brieber S, Neufang S, Bruning N, et al. (2007) Structural brain abnormalities in adolescents with autism spectrum disorder and patients with attention deficit/hyperactivity disorder. J Child Psychol Psychiatry, 48, 1251-1258.

Caldon CE, Sergio CM, Schutte J, et al. (2009) Estrogen regulation of cyclin E2 requires cyclin D1 but not c-Myc. Mol Cell Biol, 29, 4623-4639.

Canitano R (2007) Epilepsy in autism spectrum disorders. Eur Child Adolesc Psychiatry, 16, 61-66.

Carvill GL, Heavin SB, Yendle SC, et al. (2013) Targeted resequencing in epileptic encephalopathies identifies de novo mutations in CHD2 and SYNGAP1. Nat Genet, 45, 825-830.

Chai M, Sanosaka T, Okuno H, et al. (2018) Chromatin remodeler CHD7 regulates the stem cell identity of human neural progenitors. Genes Dev, 32, 165-180.

Chenier S, Yoon G, Argiropoulos B, et al. (2014) CHD2 haploinsufficiency is associated with developmental delay, intellectual disability, epilepsy and neurobehavioural problems. J Neurodev Disord, 6, 9.

Cotney J, Muhle RA, Sanders SJ, et al. (2015) The autism-associated chromatin modifier CHD8 regulates other autism risk genes during human neurodevelopment. Nat Commun, 6, 6404.

de Anda FC, Rosario AL, Durak O, et al. (2012) Autism spectrum disorder susceptibility gene TAOK2 affects basal dendrite formation in the neocortex. Nat Neurosci, 15, 1022-1031.

Donovan APA, Basson MA (2017) The neuroanatomy of autism - a developmental perspective. Journal of anatomy, 230, 4-15.

Donovan APA, Yu T, Ellegood J, et al. (2017) Cerebellar Vermis and Midbrain Hypoplasia Upon Conditional Deletion of Chd7 from the Embryonic Mid-Hindbrain Region. Frontiers in neuroanatomy, 11, 86.

Durak O, Gao F, Kaeser-Woo YJ, et al. (2016) Chd8 mediates cortical neurogenesis via transcriptional regulation of cell cycle and Wnt signaling. Nat Neurosci, 19, 1477-1488.

Dziuk MA, Gidley Larson JC, Apostu A, et al. (2007) Dyspraxia in autism: association with motor, social, and communicative deficits. Dev Med Child Neurol, 49, 734-739.

Engelen E, Akinci U, Bryne JC, et al. (2011) Sox2 cooperates with Chd7 to regulate genes that are mutated in human syndromes. Nat Genet, 43, 607-11.

Epi KC, Epilepsy Phenome/Genome P, Allen AS, et al. (2013) De novo mutations in epileptic encephalopathies. Nature, 501, 217-221.

Feng W, Kawauchi D, Korkel-Qu H, et al. (2017) Chd7 is indispensable for mammalian brain development through activation of a neuronal differentiation programme. Nat Commun, 8, 14758.

Frye RE, Casanova MF, Fatemi SH, et al. (2016) Neuropathological Mechanisms of Seizures in Autism Spectrum Disorder. Front Neurosci, 10, 192.

Fujita K, Ogawa R, Ito K (2016) CHD7, Oct3/4, Sox2, and Nanog control FoxD3 expression during mouse neural crest-derived stem cell formation. Febs j, 283, 3791-3806.

Fujita K, Ogawa R, Kawasaki S, et al. (2014) Roles of chromatin remodelers in maintenance mechanisms of multipotency of mouse trunk neural crest cells in the formation of neural crest-derived stem cells. Mech Dev, 133, 126-145.

Gage PJ, Hurd EA, Martin DM (2015) Mouse Models for the Dissection of CHD7 Functions in Eye Development and the Molecular Basis for Ocular Defects in CHARGE Syndrome. Invest Ophthalmol Vis Sci, 56, 7923-7930.

Galizia EC, Myers CT, Leu C, et al. (2015) CHD2 variants are a risk factor for photosensitivity in epilepsy. Brain, 138, 1198-1207.

Gao X, Gordon D, Zhang D, et al. (2007) CHD7 Gene Polymorphisms Are Associated with Susceptibility to Idiopathic Scoliosis. Am J Hum Genet, 80, 957-965.

Gompers AL, Su-Feher L, Ellegood J, et al. (2017) Germline Chd8 haploinsufficiency alters brain development in mouse. Nat Neurosci, 20, 1062-1073.

Harada A, Okada S, Konno D, et al. (2012) Chd2 interacts with H3.3 to determine myogenic cell fate. Embo j, 31, 2994-3007.

Helbig I, Mefford HC, Sharp AJ, et al. (2009) 15q13.3 microdeletions increase risk of idiopathic generalized epilepsy. Nat Genet, 41, 160-162.

Hendrich B, Bickmore W (2001) Human diseases with underlying defects in chromatin structure and modification. Human molecular genetics, 10, 2233-2242.

Ho L, Crabtree GR (2010) Chromatin remodelling during development. Nature, 463, 474-484.

Hurd EA, Capers PL, Blauwkamp MN, et al. (2007) Loss of Chd7 function in gene-trapped reporter mice is embryonic lethal and associated with severe defects in multiple developing tissues. Mamm Genome, 18, 94-104.

Iwase S, Martin DM (2018) Chromatin in nervous system development and disease. In Molecular and cellular neurosciences), pp. 1-3.

Janssen N, Bergman JE, Swertz MA, et al. (2012) Mutation update on the CHD7 gene involved in CHARGE syndrome. Hum Mutat, 33, 1149-1160.

Jones KM, Saric N, Russell JP, et al. (2015) CHD7 maintains neural stem cell quiescence and prevents premature stem cell depletion in the adult hippocampus. Stem Cells, 33, 196-210.

Jongmans MC, van Ravenswaaij-Arts CM, Pitteloud N, et al. (2009) CHD7 mutations in patients initially diagnosed with Kallmann syndrome--the clinical overlap with CHARGE syndrome. Clin Genet, 75, 65-71.

Katayama Y, Nishiyama M, Shoji H, et al. (2016) CHD8 haploinsufficiency results in autistic-like phenotypes in mice. Nature, 537, 675-679.

Kim HG, Kurth I, Lan F, et al. (2008) Mutations in CHD7, encoding a chromatin-remodeling protein, cause idiopathic hypogonadotropic hypogonadism and Kallmann syndrome. Am J Hum Genet, 83, 511-519.

Kobayashi M, Kishida S, Fukui A, et al. (2002) Nuclear localization of Duplin, a beta-catenin-binding protein, is essential for its inhibitory activity on the Wnt signaling pathway. J Biol Chem, 277, 5816-5822.

Kulkarni S, Nagarajan P, Wall J, et al. (2008) Disruption of chromodomain helicase DNA binding protein 2 (CHD2) causes scoliosis. Am J Med Genet A, 146a, 1117-1127.

Lado FA, Rubboli G, Capovilla G, et al. (2013) Pathophysiology of epileptic encephalopathies. Epilepsia, 54 Suppl 8, 6-13.

Lebrun N, Parent P, Gendras J, et al. (2017) Autism spectrum disorder recurrence, resulting of germline mosaicism for a CHD2 gene missense variant. Clin Genet, 92, 669-670.

Leyfer OT, Folstein SE, Bacalman S, et al. (2006) Comorbid psychiatric disorders in children with autism: interview development and rates of disorders. J Autism Dev Disord, 36, 849-861.

Liu JC, Ferreira CG, Yusufzai T (2015) Human CHD2 is a chromatin assembly ATPase regulated by its chromo- and DNA-binding domains. J Biol Chem, 290, 25-34.

Liu YQ, Yu F, Liu WH, et al. (2014) Dysfunction of hippocampal interneurons in epilepsy. Neurosci Bull, 30, 985-998.

Luijsterburg MS, de Krijger I, Wiegant WW, et al. (2016) PARP1 Links CHD2-Mediated Chromatin Expansion and H3.3 Deposition to DNA Repair by Non-homologous End-Joining. Mol Cell, 61, 547-562.

Lund C, Brodtkorb E, Oye AM, et al. (2014) CHD2 mutations in Lennox-Gastaut syndrome. Epilepsy Behav, 33, 18-21.

Marfella CG, Henninger N, LeBlanc SE, et al. (2008) A mutation in the mouse Chd2 chromatin remodeling enzyme results in a complex renal phenotype. Kidney Blood Press Res, 31, 421-432.

Marfella CG, Ohkawa Y, Coles AH, et al. (2006) Mutation of the SNF2 family member Chd2 affects mouse development and survival. J Cell Physiol, 209, 162-171.

Marfella CGA, Imbalzano AN (2007) The Chd family of chromatin remodelers. Mutation research, 618, 30-40.

Meganathan K, Lewis EMA, Gontarz P, et al. (2017) Regulatory networks specifying cortical interneurons from human embryonic stem cells reveal roles for CHD2 in interneuron development. Proc Natl Acad Sci U S A, 114, E11180-e11189.

Merner N, Forgeot d'Arc B, Bell SC, et al. (2016) A de novo frameshift mutation in chromodomain helicase DNA-binding domain 8 (CHD8): A case report and literature review. Am J Med Genet A.

Nagarajan P, Onami TM, Rajagopalan S, et al. (2009) Role of chromodomain helicase DNA-binding protein 2 in DNA damage response signaling and tumorigenesis. Oncogene, 28, 1053-1062.

Neale BM, Kou Y, Liu L, et al. (2012) Patterns and rates of exonic de novo mutations in autism spectrum disorders. Nature, 485, 242-245.

Nishiyama M, Nakayama K, Tsunematsu R, et al. (2004) Early embryonic death in mice lacking the beta-catenin-binding protein Duplin. Mol Cell Biol, 24, 8386-8394.

Nishiyama M, Oshikawa K, Tsukada Y, et al. (2009) CHD8 suppresses p53-mediated apoptosis through histone H1 recruitment during early embryogenesis. Nat Cell Biol, 11, 172-182.

Nishiyama M, Skoultchi AI, Nakayama KI (2012) Histone H1 recruitment by CHD8 is essential for suppression of the Wnt-beta-catenin signaling pathway. Mol Cell Biol, 32, 501-512.

Okuno H, Renault Mihara F, Ohta S, et al. (2017) CHARGE syndrome modeling using patient-iPSCs reveals defective migration of neural crest cells harboring CHD7 mutations. Elife, 6.

O'Roak BJ, Stessman HA, Boyle EA, et al. (2014) Recurrent de novo mutations implicate novel genes underlying simplex autism risk. Nat Commun, 5, 5595.

O'Roak BJ, Vives L, Girirajan S, et al. (2012) Sporadic autism exomes reveal a highly interconnected protein network of de novo mutations. Nature, 485, 246-250.

Parikshak N, Luo R, Zhang A, et al. (2013) Integrative functional genomic analyses implicate specific molecular pathways and circuits in autism. Cell, 155, 1008-1021.

Patten SA, Jacobs-McDaniels NL, Zaouter C, et al. (2012) Role of Chd7 in zebrafish: a model for CHARGE syndrome. PLoS One, 7, e31650.

Pinto AM, Bianciardi L, Mencarelli MA, et al. (2016) Exome sequencing analysis in a pair of monozygotic twins re-evaluates the genetics behind their intellectual disability and reveals a CHD2 mutation. Brain Dev, 38, 590-596.

Platt RJ, Zhou Y, Slaymaker IM, et al. (2017) Chd8 Mutation Leads to Autistic-like Behaviors and Impaired Striatal Circuits. Cell Rep, 19, 335-350.

Prasad MS, Sauka-Spengler T, LaBonne C (2012) Induction of the neural crest state: control of stem cell attributes by gene regulatory, post-transcriptional and epigenetic interactions. Dev Biol, 366, 10-21.

Rajagopalan S, Nepa J, Venkatachalam S (2012) Chromodomain helicase DNA-binding protein 2 affects the repair of X-ray and UV-induced DNA damage. Environ Mol Mutagen, 53, 44-50.

Riedel G, Micheau J (2001) Function of the hippocampus in memory formation: desperately seeking resolution. Prog Neuropsychopharmacol Biol Psychiatry, 25, 835-853.

Rodriguez D, Bretones G, Quesada V, et al. (2015) Mutations in CHD2 cause defective association with active chromatin in chronic lymphocytic leukemia. Blood, 126, 195-202.

Rodriguez-Paredes M, Ceballos-Chavez M, Esteller M, et al. (2009) The chromatin remodeling factor CHD8 interacts with elongating RNA polymerase II and controls expression of the cyclin E2 gene. Nucleic Acids Res, 37, 2449-2460.

Ronan JL, Wu W, Crabtree GR (2013) From neural development to cognition: unexpected roles for chromatin. Nature reviews. Genetics, 14, 347-359.

Sakamoto I, Kishida S, Fukui A, et al. (2000) A novel beta-catenin-binding protein inhibits beta-catenin-dependent Tcf activation and axis formation. J Biol Chem, 275, 32871-32878.

Sanders SJ, Murtha MT, Gupta AR, et al. (2012) De novo mutations revealed by whole-exome sequencing are strongly associated with autism. Nature, 485, 237-241.

Semba Y, Harada A, Maehara K, et al. (2017) Chd2 regulates chromatin for proper gene expression toward differentiation in mouse embryonic stem cells. Nucleic Acids Res, 45, 8758-8772.

Shen T, Ji F, Yuan Z, et al. (2015) CHD2 is Required for Embryonic Neurogenesis in the Developing Cerebral Cortex. Stem Cells, 33, 1794-1806.

Stolerman ES, Smith B, Chaubey A, et al. (2016) CHD8 intragenic deletion associated with autism spectrum disorder. Eur J Med Genet.

Suetterlin P, Hurley S, Mohan C, et al. (2018) Altered Neocortical Gene Expression, Brain Overgrowth and Functional Over-Connectivity in Chd8 Haploinsufficient Mice. Cereb Cortex.

Sugathan A, Biagioli M, Golzio C, et al. (2014) CHD8 regulates neurodevelopmental pathways associated with autism spectrum disorder in neural progenitors. Proc Natl Acad Sci U S A, 111, E4468-77.

Suls A, Jaehn JA, Kecskes A, et al. (2013) De novo loss-of-function mutations in CHD2 cause a fever-sensitive myoclonic epileptic encephalopathy sharing features with Dravet syndrome. Am J Hum Genet, 93, 967-975.

Takada I, Mihara M, Suzawa M, et al. (2007) A histone lysine methyltransferase activated by non-canonical Wnt signalling suppresses PPAR-gamma transactivation. Nat Cell Biol, 9, 1273-1285.

Talkowski ME, Rosenfeld JA, Blumenthal I, et al. (2012) Sequencing chromosomal abnormalities reveals neurodevelopmental loci that confer risk across diagnostic boundaries. Cell, 149, 525-537.

Taurines R, Schwenck C, Westerwald E, et al. (2012) ADHD and autism: differential diagnosis or overlapping traits? A selective review. Atten Defic Hyperact Disord, 4, 115-139.

Thompson BA, Tremblay V, Lin G, et al. (2008) CHD8 is an ATP-dependent chromatin remodeling factor that regulates beta-catenin target genes. Mol Cell Biol, 28, 3894-3904.

Van de Laar I, Dooijes D, Hoefsloot L, et al. (2007) Limb anomalies in patients with CHARGE syndrome: an expansion of the phenotype. Am J Med Genet A, 143a, 2712-2715.

Vissers LE, van Ravenswaaij CM, Admiraal R, et al. (2004) Mutations in a new member of the chromodomain gene family cause CHARGE syndrome. Nat Genet, 36, 955-957.

Wang P, Lin M, Pedrosa E, et al. (2015) CRISPR/Cas9-mediated heterozygous knockout of the autism gene CHD8 and characterization of its transcriptional networks in neurodevelopment. Mol Autism, 6, 55.

Wang T, Guo H, Xiong B, et al. (2016) De novo genic mutations among a Chinese autism spectrum disorder cohort. Nat Commun, 7, 13316.

Whittaker DE, Kasah S, Donovan APA, et al. (2017) Distinct cerebellar foliation anomalies in a CHD7 haploinsufficient mouse model of CHARGE syndrome. Am J Med Genet C Semin Med Genet, 175.

Whittaker DE, Riegman KL, Kasah S, et al. (2017) The chromatin remodeling factor CHD7 controls cerebellar development by regulating reelin expression. J Clin Invest, 127, 874-887.

Wilkinson B, Grepo N, Thompson BL, et al. (2015) The autism-associated gene chromodomain helicase DNA-binding protein 8 (CHD8) regulates noncoding RNAs and autism-related genes. Transl Psychiatry, 5, e568.

Yamamoto T, Takenaka C, Yoda Y, et al. (2018) Differentiation potential of Pluripotent Stem Cells correlates to the level of CHD7. Sci Rep, 8, 241.

Yates JA, Menon T, Thompson BA, et al. (2010) Regulation of HOXA2 gene expression by the ATP-dependent chromatin remodeling enzyme CHD8. FEBS Lett, 584, 689-693.

Yu T, Meiners LC, Danielsen K, et al. (2013) Deregulated FGF and homeotic gene expression underlies cerebellar vermis hypoplasia in CHARGE syndrome. Elife, 2, e01305.

Yuan CC, Zhao X, Florens L, et al. (2007) CHD8 associates with human Staf and contributes to efficient U6 RNA polymerase III transcription. Mol Cell Biol, 27, 8729-8738.

Zahir F, Firth HV, Baross A, et al. (2007) Novel deletions of 14q11.2 associated with developmental delay, cognitive impairment and similar minor anomalies in three children. J Med Genet, 44, 556-561.

Figure legends

Figure 1. Distinct *Chd8, Chd7* and *Chd2* expression patterns at E12.5.

In situ hybridisation on sagittal sections of mouse embryos at developmental stage E12.5 using antisense riboprobes to detect *Chd8, Chd7* and *Chd2* mRNA, anterior to the right (A-C). Gene expression is indicated by purple/blue staining. Note the widespread *Chd8* expression in most embryonic tissues (A), the high, localized expression of *Chd7*, specifically in the developing nervous system (B), and very low, widespread expression of *Chd2* (C). High magnification images of the developing cerebellum (Aa-Ca) demonstrate the presence of *Chd8* (Aa) and *Chd7* (Ba) transcripts throughout the neuroepithelium, with little *Chd2* expression evident (Ca). High magnification images through the neocortex show widespread *Chd8* expression (Ab), note that *Chd7* expression tends to be higher on the ventricular side (Bb) and that there is little discernible *Chd2* expression (Cb). Other regions with relatively strong signals were the nasal epithelium, tail, genital tubercle, intersomitic mesoderm, spinal cord, mid brain, diencephalon, tongue and pituitary. Scale bars represent 100 μm.

Cb = cerebellum; Di = diencephalon; Drg = dorsal root ganglia; FP = floor plate; Gt = genital tubercle; Gu = gut; H = heart; Is = isthmus; Iso = intersomitic mesoderm; Lu = lungs; LRL = lower rhombic lip; MB = midbrain; MZ = molecular zone; NC = neocortex; Pi = pituitary; Sc = spinal cord; SVZ = subventricular zone; Ta = tail; To = tongue; URL = upper rhombic lip; VZ = ventricular zone.

Figure 2. *Chd7* and *Chd8* are expressed in multiple organs at E12.5.

In situ hybridisation images of *Chd8* (A-E) and *Chd7* (F-I) transcripts around the cochlea of the inner ear (A, F), kidney (B, G), lung (C, H) eye (D, I) and tooth (E, J). Scale bars represent 100 μm.

C = cornea; CD = cochlear duct: CVG = cochlea-vestibular ganglia; CM = condensing mesenchyme; LE = lung epithelium; LN = lens; MT = metanephric tubule; NR = neuroretina; PI = primordium of incisor; PO = pre-optic cup; RPE = retinal pigmented epithelium; SB = segmental bronchus.

Figure 3. Distinct nervous system and organ-specific expression patterns of *Chd8, Chd7 and Chd2* in E14.5 mouse embryos.

In situ hybridisation on sagittal sections of E14.5 mouse embryos (A-C), anterior to the right. Note distinct *Chd8, Chd7* and *Chd2* expression patterns throughout the embryos with notably higher level in the developing nervous system. Beyond the nervous system, other notable regions of expression included various organs and glands, for example the thymus and thyroid, heart and kidneys. High magnification images (Aa-Ce) revealed specific expression patterns in the cerebellum (Aa-Ca), Neocortex (Ab-Cb), Eye (Ac-Cc), Lung (Ad-Cd) and kidney (Ae-Ce). Scale bars represent 100 μm.

B = bronchus; C = cornea; Cb = cerebellum; CD = collecting duct; CM = condensing mesenchyme; CP = choroid plexus; C-PL = cortical plate; Di = diencephalon; Dh = digit of hindlimb; GE = gastric epithelium; GEm = ganglionic eminence; Gu = gut; H = heart; K = kidney; LC = lens capsule; LE = lung epithelium; Li = liver; LN = lens; Lu = lung; Mb = mid brain roof plate; MZ = marginal zone; NC = neocortex; NR = neural retina; OE = olfactory epithelium; ON = optic nerve and surrounding structures; PO = pre-optic cup; RL = rhombic lip; RPE = retinal pigmented epithelium; Sc = spinal cord; T = thyroid ; To = tongue; Ta = tail; Th = thymus; TG = trigeminal ganglion; vI = ventral incisor; VZ = ventricular zone.

Figure 4. Comparative *Chd8*, *Chd7* and *Chd2* expression patterns in the newborn mouse brain.

Sagittal sections through newborn mouse brain (anterior to the right), hybridised with antisense RNA probes to detect *Chd8* (A, A'), *Chd7* (B, B') and *Chd2* (C, C') transcripts in blue. Note wide-spread expression of Chd8, highly localised Chd7 expression in the cerebellum and pons, and Chd2 in the neocortex, midbrain and cerebellum. High magnification views of the cerebellum (Aa-Ca) and neocortex (Ab-Cb) are shown. Scale bars represent 100 μm.

Cb = cerebellum; EGL = external granule cell layer; HC = hippocampus; Hy = hypothalamus; I = cortical layer I; II-III = cortical layers II-III; IC = inferior colliculus; IGL, = internal granule cell layer; Me = medulla; NC = neocortex; OB = olfactory bulb; Pn = pons; SC = superior colliculus; SOC = superior olivary complex.

Figure 5. *Chd8, Chd7* and *Chd2* are expressed in the early postnatal cerebellum, hippocampus, neocortex and rostral migratory stream.

Sagittal sections through postnatal day 7 (P7) mouse brain (anterior to the right), hybridised with antisense RNA probes to detect *Chd8* (A, A'), *Chd7* (B, B') and *Chd2* (C, C') transcripts, visualised in blue. Higher magnification images to visualise specific expression domains in the cerebellum (Aa-Ac), hippocampus (Ba-Bc), and neocortex (Ca-Cc) are shown. Scale bars represent 100 μm.

CA1-3 = cornu ammonis 1-3; Cb = cerebellum; DG = dentate gyrus; EGL = external granule cell layer; GL = glomerular layer; HC = hippocampus; I = cortical layer I; II-III = cortical layers II-III; IGL = internal granule cell layer; IPL = internal plexiform layer; ML = molecular layer; NC = neocortex; OB = olfactory bulb; RMS = rostral migratory stream; SGZ = subgranular zone; WM = white matter.

Figure 6. Comparison of *Chd8, Chd7* and *Chd2* expression patterns in the P20 mouse brain.

Sagittal sections through P20 mouse brain (anterior to the right), hybridised with antisense RNA probes to detect *Chd8* (A, A'), *Chd7* (B, B') and *Chd2* (C, C') transcripts, visualised in blue. Note high expression of all three genes in the cerebellum, with widespread *Chd8* and *Chd2* expression remaining in the neocortex. High magnification images of the cerebellum (Aa-Ca); hippocampus (Ab-Cb) and neocortex (Ac-Cc) are shown. Scale bars represent 100 μm.

CA1-3 = cornu ammonis 1-3; Cb = cerebellum; DG = dentate gyrus; GCL = granule cell layer; HC = hippocampus; I = cortical layer I; II-III = cortical layers II-III; ML = molecular layer; NC = neocortex; OB = olfactory bulb; RMS = rostral migratory stream; SGZ = subgranular zone; WM, = white matter.

Supplementary Figure 1. Distinct *Chd8* and *Chd7* expression patterns within the neural tube at E12.5.

In situ hybridisation on sagittal (anterior to the right) and transverse sections of mouse embryos at developmental stage E12.5 using antisense riboprobes to detect *Chd8* and *Chd7* mRNA (A-H). Gene expression is indicated by purple/blue staining. Note that both *Chd8* and *Chd7* are expressed throughout the length of the neural tube (A, B, E, F). Whilst *Chd8* displays no mediolateral or dorsoventral gradient in transverse sections *Chd7* shows distinct enrichment in the ventricular zone of the developing CNS and a ventral to dorsal gradient within the spinal cord.

Drg = dorsal root ganglia; Iso = intersomitic region; LGE = lateral ganglionic eminence; MGE = medial ganglionic eminence; No = notochord; NT = neural tube; SE = surface ectoderm.

Supplementary Figure 2. Sense control sections at E12.5.

In situ hybridisation on sagittal (anterior to the right) sections of mouse embryos at developmental stage E12.5 using sense riboprobes to *Chd8, Chd7* and *Chd2* mRNA. Note that for all three genes there is little to no hybridisation or staining using the sense riboprobe in contrast to what is seen when using the anti-sense probe.

1

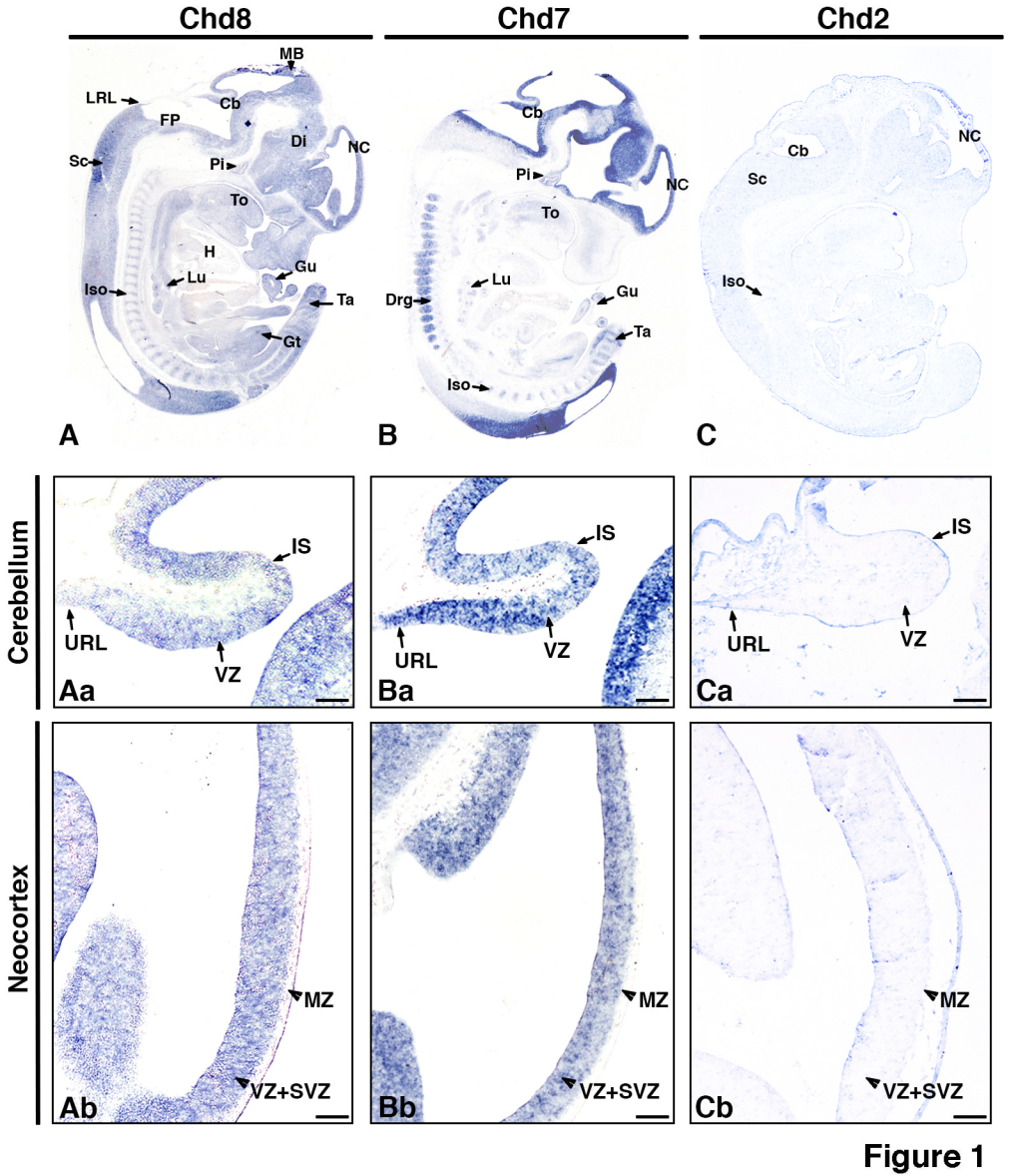
Chd8
Chd7
Chd2
MB
LRL
Cb
FP
Di
NC
Sc
Pi
To
H
Gu
Lu
Iso
Ta
Gt
Drg
A
B
C
Cerebellum
Neocortex
IS
URL
VZ
MZ
VZ+SVZ
Aa
Ba
Ca
Ab
Bb
Cb

Figure 1

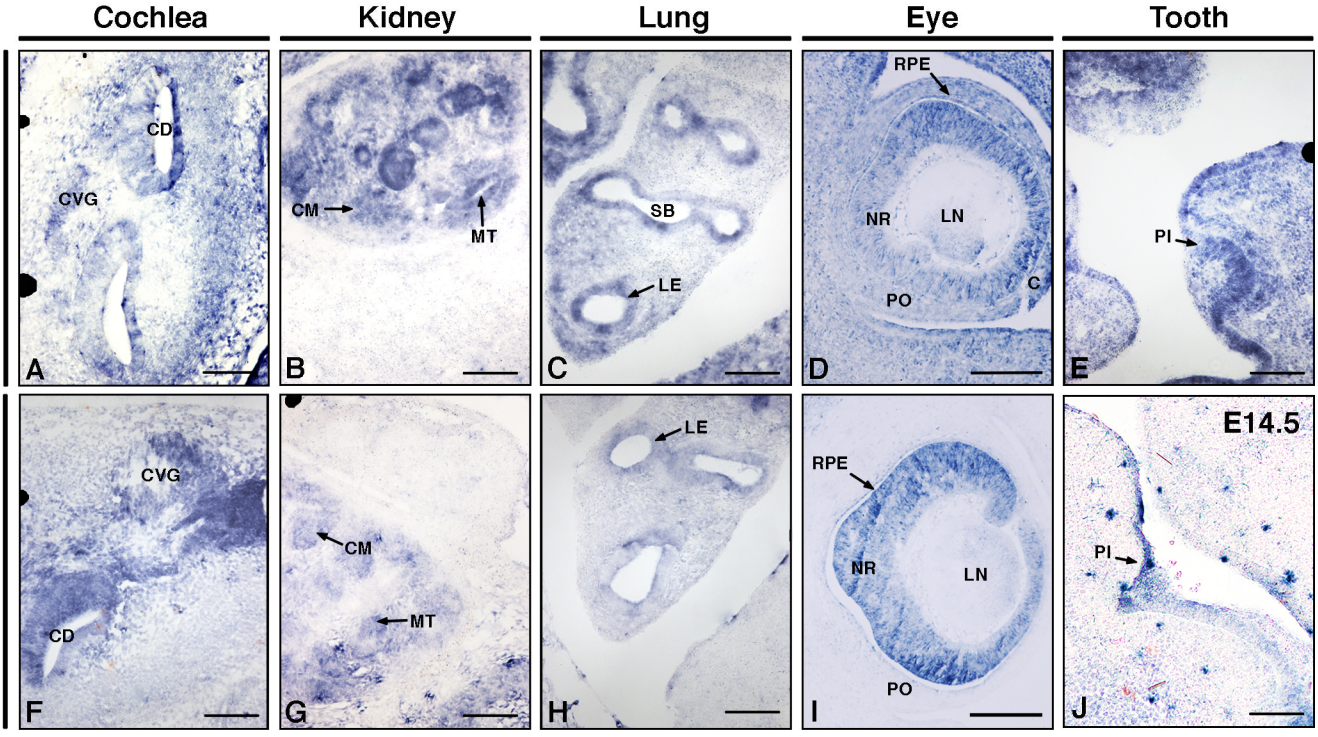
Cochlea
Kidney
Lung
Eye
Tooth
Chd8
Chd7
CD
CVG
CM
MT
SB
LE
RPE
NR
LN
PO
C
PI
E14.5
A
B
C
D
E
F
G
H
I
J

Figure 2

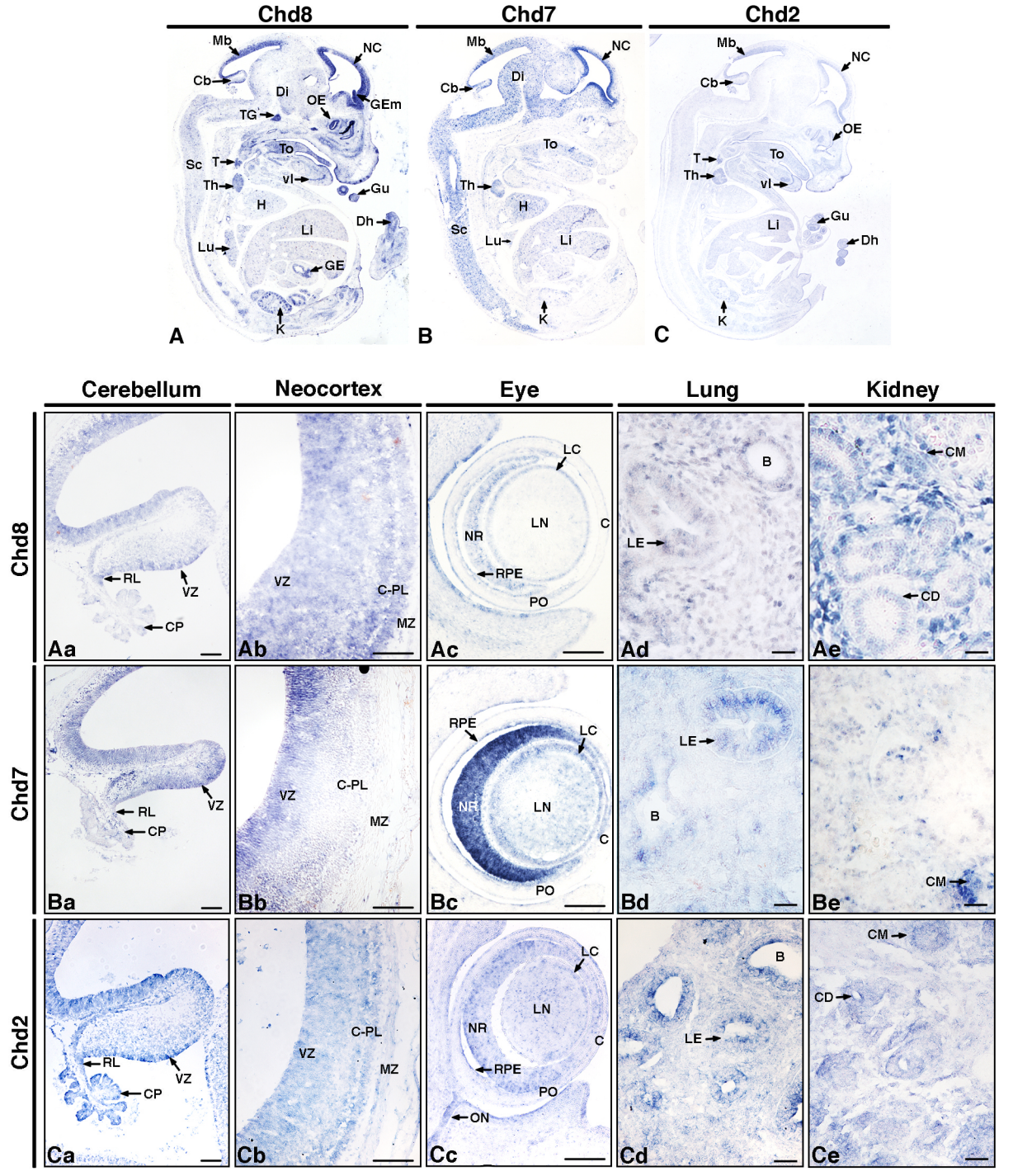
Chd8
Chd7
Chd2
Mb
NC
Cb
Di
OE
GEm
TG
To
Sc
T
vl
Th
Gu
H
Li
Dh
Lu
GE
K
A
B
C
Cerebellum
Neocortex
Eye
Lung
Kidney
RL
VZ
CP
C-PL
MZ
LC
LN
NR
RPE
PO
C
LE
B
CM
CD
ON
Aa
Ab
Ac
Ad
Ae
Ba
Bb
Bc
Bd
Be
Ca
Cb
Cc
Cd
Ce

Figure 3

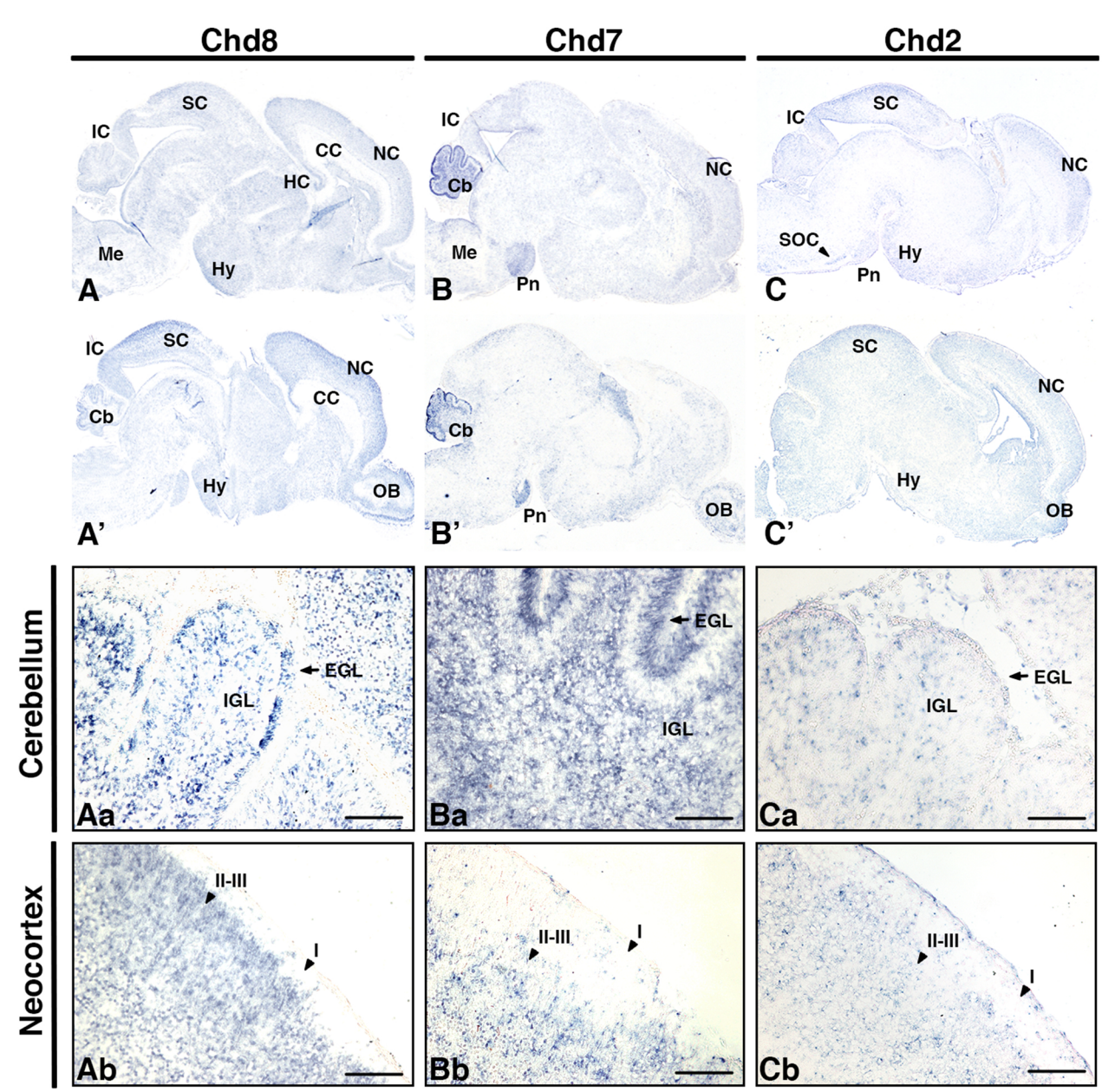
Chd8
Chd7
Chd2
SC
IC
CC
NC
HC
Me
Hy
A
Cb
Pn
B
SOC
C
OB
A'
B'
C'
Cerebellum
Neocortex
EGL
IGL
Aa
Ba
Ca
II-III
I
Ab
Bb
Cb

Figure 4

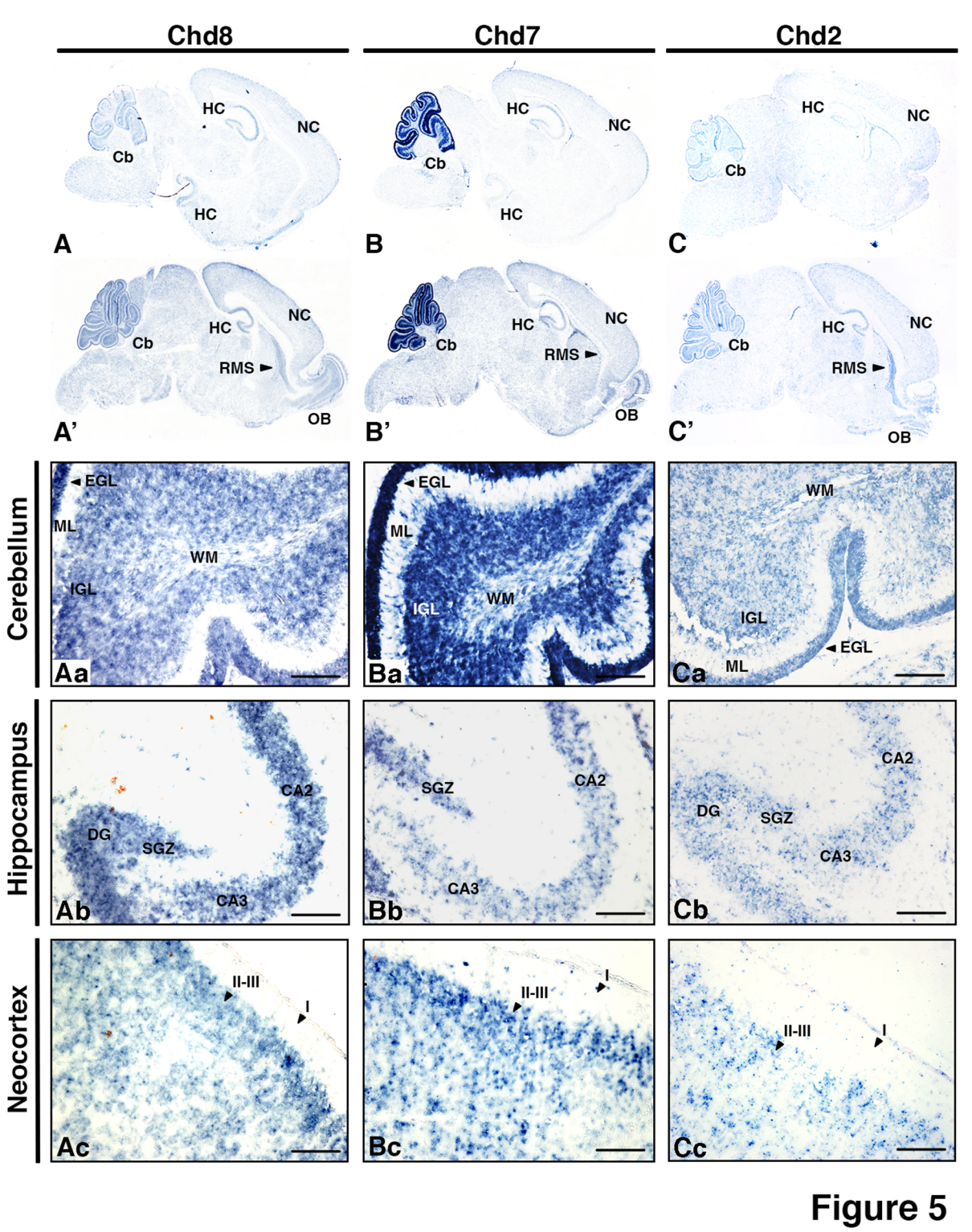
Chd8
Chd7
Chd2
HC
NC
Cb
A
B
C
RMS
OB
A'
B'
C'
Cerebellum
EGL
ML
WM
IGL
Aa
Ba
Ca
Hippocampus
CA2
DG
SGZ
CA3
Ab
Bb
Cb
Neocortex
II-III
I
Ac
Bc
Cc

Figure 5

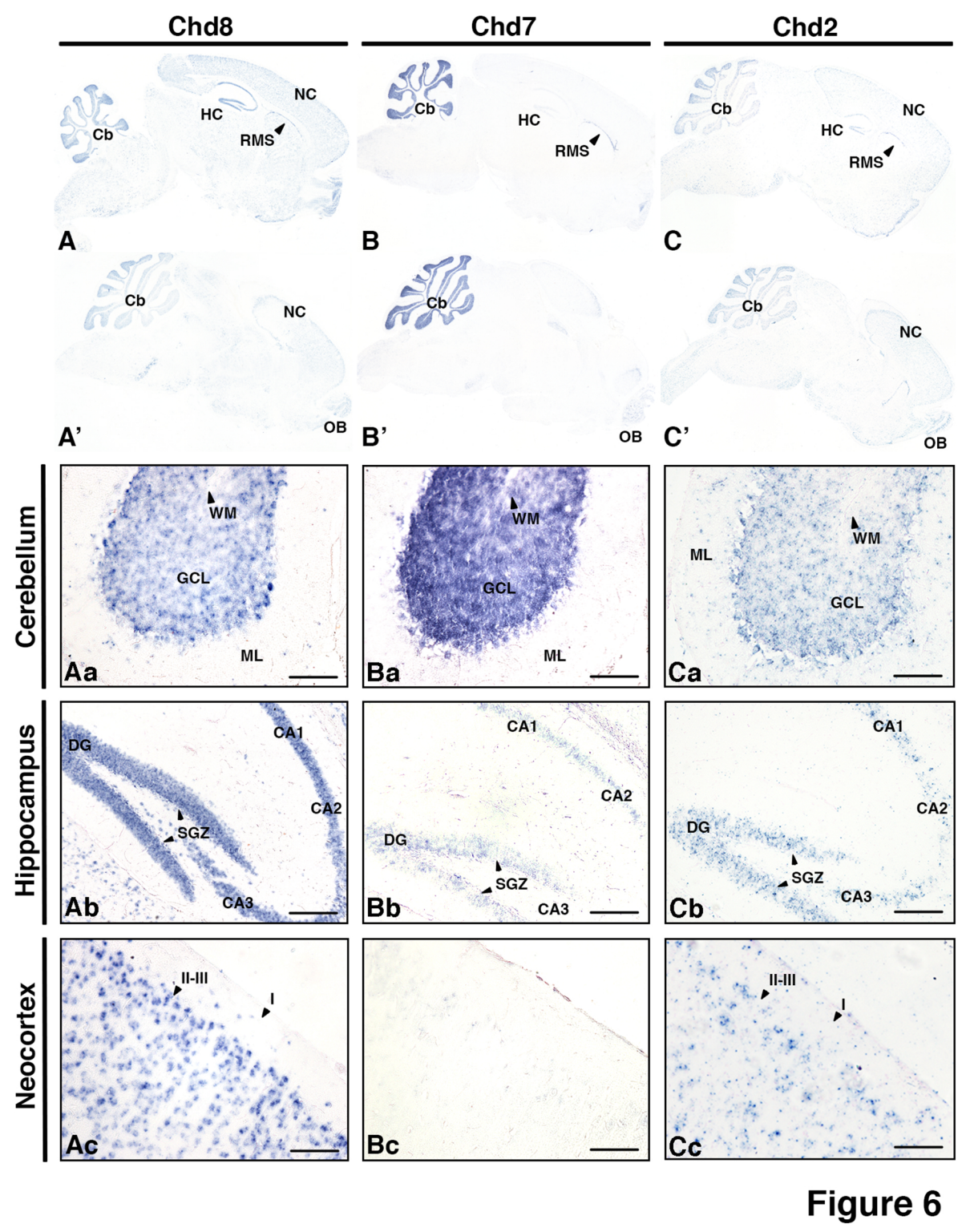
Chd8
Chd7
Chd2
Cb
HC
NC
RMS
A
B
C
OB
A'
B'
C'
Cerebellum
Hippocampus
Neocortex
WM
GCL
ML
Aa
Ba
Ca
DG
CA1
CA2
CA3
SGZ
Ab
Bb
Cb
II-III
I
Ac
Bc
Cc

Figure 6

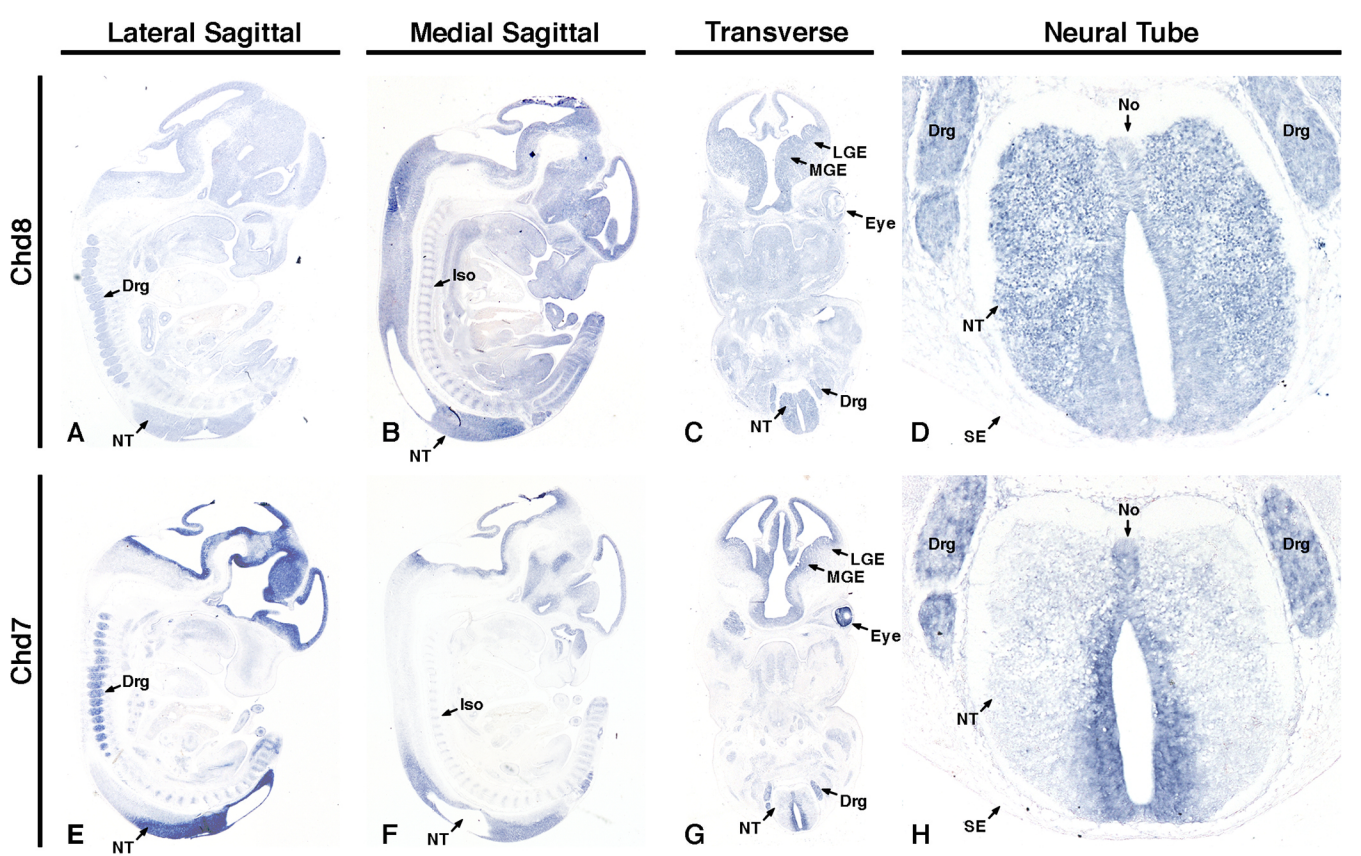

Supplementary Figure 1

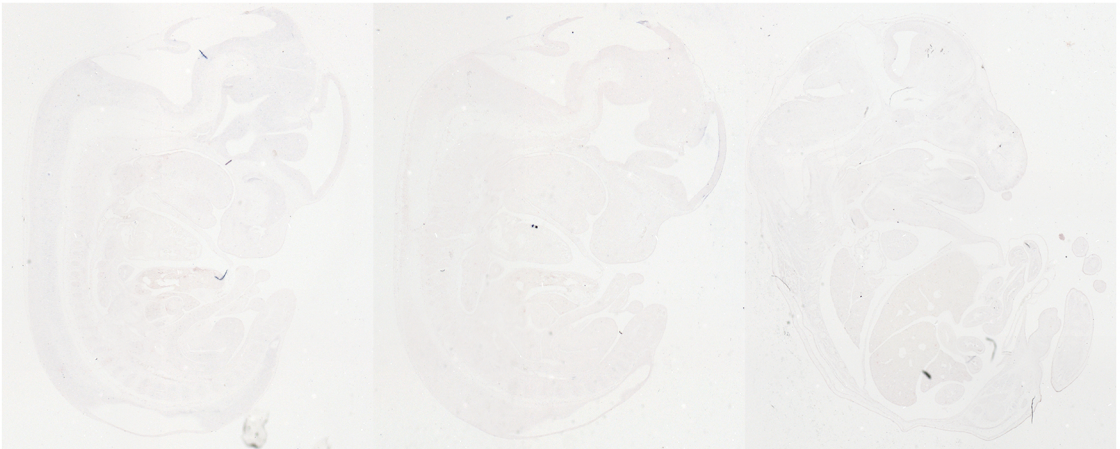

Supplementary Figure 2